Army Research Laboratory

Asymptotic Techniques for Atomic Waveguide Calculations

by William M. Golding

ARL-TR-5343 **September 2010**

NOTICES

Disclaimers

Army Research Laboratory
Adelphi, MD 20783-1197

ARL-TR-5343 September 2010

Asymptotic Techniques for Atomic Waveguide Calculations

William M. Golding
Sensors and Electron Devices Directorate, ARL

REPORT DOCUMENTATION PAGE	*Form Approved* *OMB No. 0704-0188*

1. REPORT DATE *(DD-MM-YYYY)*	2. REPORT TYPE	3. DATES COVERED (From - To)
September 2010	Final	

4. TITLE AND SUBTITLE Asymptotic Techniques for Atomic Waveguide Calculations	5a. CONTRACT NUMBER 5b. GRANT NUMBER 5c. PROGRAM ELEMENT NUMBER
6. AUTHOR(S) William M. Golding	5d. PROJECT NUMBER 5e. TASK NUMBER 5f. WORK UNIT NUMBER
7. PERFORMING ORGANIZATION NAME(S) AND ADDRESS(ES) U.S. Army Research Laboratory ATTN: RDRL-SEE-O 2800 Powder Mill Road Adelphi MD 20783-1197	8. PERFORMING ORGANIZATION REPORT NUMBER ARL-TR-5343
9. SPONSORING/MONITORING AGENCY NAME(S) AND ADDRESS(ES)	10. SPONSOR/MONITOR'S ACRONYM(S) 11. SPONSOR/MONITOR'S REPORT NUMBER(S)

12. DISTRIBUTION/AVAILABILITY STATEMENT

Approved for public release; distribution unlimited.

13. SUPPLEMENTARY NOTES

14. ABSTRACT

Asymptotic expansions describing the behavior of the radial wavefunctions of a magnetic atomic waveguide are developed. In this system, some components of the spinor wavefunctions do not die off exponentially and are therefore significant at large distances. This is related to the quasibound nature of the system. A good representation of the nondecaying components of the eigenstates at large distances from the guide center is required so that the calculated eigenstates can be used reliably in further numerical calculations. The asymptotic expansions presented here provide this representation and are readily related to the power series solutions developed in ARL-TR-5335. By connecting those power series solutions to the asymptotic expansions developed here, an efficient representation of the exact radial wavefunctions can be obtained. These wavefunctions are needed for detailed studies of important properties of magnetic guides such as; sensitivity to noise driven spin flips, importance of quantum Majorana transitions, energy level dependence on magnetic field, the effects of guiding field imperfections as well as the onset and departure of adiabatic behavior.

15. SUBJECT TERMS

Atomic waveguide, eigenstate calculation, asymptotic expansions, phase integral technique

16. SECURITY CLASSIFICATION OF:			17. LIMITATION OF ABSTRACT	18. NUMBER OF PAGES	19a. NAME OF RESPONSIBLE PERSON
a. REPORT	b. ABSTRACT	c. THIS PAGE			William M. Golding
Unclassified	Unclassified	Unclassified	UU	24	19b. TELEPHONE NUMBER (*Include area code*) (301) 394-1535

Standard Form 298 (Rev. 8/98)
Prescribed by ANSI Std. Z39.18

Contents

INTENTIONALLY LEFT BLANK.

1. Introduction

In this work, radial wavefunctions describing the quantum behavior of a spin one-half particle far from the center of a uniform atomic waveguide are formulated. The model waveguide potential is an ideal transverse quadrupole magnetic field that extends to infinite distances and is unbounded in magnitude. The spin of the particle can be considered in either a global basis or in a local basis. The quantization axis for the global basis is directed in the z-direction along the axis of the guide while the quantization axis for the local basis is taken to be directed everywhere along the local direction of the quadrupole magnetic field. In either basis, the atomic wavefunction has two components one of which might seem more “trapped” than the other. However, in each of these bases there is a significant component of the spinor eigenstates that extends to infinity and represents the amplitude for an atom to be found outside of the trapping region of the waveguide.

The asymptotic solutions developed here describe the behavior of the radial wavefunctions at distances far from the guide center and thus provide a means of extending the series solutions derived in Golding (2010) to these regions. The combination of the two series can be combined into an efficient and complete solution to the waveguide eigenstate problem.

In the global spin basis, both spinor components of the radial solution appear to be unbound. They oscillate and only gradually decay along the radial direction outward towards infinity. However, in the local spin basis one component of the spinor appears to be bound and the other component appears unbound. This results from a nearly exact cancellation of the global components far from the center when viewed in the local basis. This behavior is clearly related to the adiabatic approaches often used to describe these waveguides when the axial bias field is made large (Sukumar, 1997; Brink 2007). In the adiabatic approach, the unbound component is effectively considered to be uncoupled from the bound component and ignored in a first approximation.

A goal of our research is to precisely understand the behavior of atoms guided on atom chips and moving through atom chip devices. A complete description of the solution to the waveguide problem is a required starting point in the pursuit of this goal.

This report begins by laying out the radial equations that must be solved to describe the transverse modes of an atom guide. The leading behavior of the solutions to these equations at large distances is then developed. To properly connect the four solutions that represent the leading behavior the phase integral technique is used. The phase integral technique essentially produces the relative phase and amplitudes needed to create an asymptotic expansion that correctly represents the known analytical properties that the series solution has at large distances,

where the series cannot simply be summed. In the last section, the techniques used to find the full asymptotic expansion are described.

2. Development of the Radial Equations

The equations for the radial wave functions of the quadrupole guide are derived by making use of the angular symmetry of the quadrupole magnetic field. This symmetry is expressed as the conservation of alignment, $\Lambda_z \equiv L_z - S_z$ (Golding, 2009; Hinds, 2001; Lesanovsky, 2004). The approach taken here is to find eigenfunctions that are common to both the Hamiltonian, H and the alignment, Λ_z. This method effectively separates the angular and radial dependence of the problem leaving only a coupled system of radial equations to solve.

By removing the angular dependence, the following pair of coupled radial equations for the specific alignment, μ; energy, ε; bias field, b_0; and field gradient, b_1, can be derived:

$$\begin{aligned}
\partial_\rho^2 R_+ + \frac{1}{\rho}\partial_\rho R_+ - \frac{(\mu+1/2)^2}{\rho^2}R_+ + (\varepsilon + b_0)R_+ &= b_1 \rho R_-, \\
\partial_\rho^2 R_- + \frac{1}{\rho}\partial_\rho R_- - \frac{(\mu-1/2)^2}{\rho^2}R_- + (\varepsilon - b_0)R_- &= b_1 \rho R_+.
\end{aligned} \tag{1}$$

The parameters and physical relevance of these equations have been described previously by Golding (2009). In the case of a spin half particle with integral orbital angular momentum, the pair must be solved for the allowed half-integral values of the alignment, $\mu = \pm\frac{1}{2}, \pm\frac{3}{2}, \pm\frac{5}{2}\cdots$, although the solutions for negative alignment are simply derived using symmetry when the bias field, b_0 is zero.

An important aspect of these equations is that they are coupled. In system 1, R_+ and R_- occur in both equations. In other studies of this system it is assumed that the boundary conditions at the origin can be determined by using the fact that as $\rho \to 0$ the terms on the right hand side of system 1 can be ignored (Hinds, 2000; Lesanovsky,2004; Potvliege,2001). This is equivalent to assuming that b_1 can be set to zero and limiting the results to small radii. Using this assumption it would appear that the two equations reduce to an uncoupled pair of second order differential equations for a small region near the origin. This is a type of singular perturbation since the form of the equations changes drastically when the small parameter b_1 is set to zero.

Physically, setting b_1 to zero is like turning off the trapping fields. The boundary conditions for the singular case of $b_1 = 0$ must be those of a free particle in which the spin components are completely uncoupled. Free particle states are eigenstates of the spin operator, S_z but they are

not eigenstates of the full Hamiltonian. In order to get the proper boundary conditions when the trapping fields are on, it is important to first uncouple the equations and perform a power series analysis on the resulting fourth order differential equation using the Frobenius method. The resulting series solution is evaluated at the origin and the behavior near the regular singularity is then handled correctly without making the assumption that $b_1 = 0$.

3. Uncoupled Equations

The system of radial equations displayed in system 1 contains an irregular singularity at infinity. In order to develop an asymptotic series for large values of the radius, the same decoupled fourth order equations that are developed to study the behavior near the origin are used. By solving the top equation of system 1 for R_- and substituting this result into the bottom equation, the system is uncoupled to produce the following fourth order differential equation for R_+,

$$\begin{aligned}&\rho^4 \frac{d^4}{d\rho^4} R_+ + \\ &\left[2\rho^4\varepsilon - \left(\frac{5}{2} + 2\mu^2\right)\rho^2\right]\frac{d^2}{d\rho^2} R_+ + \\ &\left[-2\rho^3 b_0 + \left(5 + 4\mu^2 + 6\mu\right)\rho\right]\frac{d}{d\rho} R_+ + \\ &\left[-b_1^2\rho^6 + \left(\varepsilon^2 - b_0^2\right)\rho^4 + \left(b_0 - 2\mu^2\varepsilon + 2\mu b_0 + \frac{1}{2}\varepsilon\right)\rho^2 - \frac{19}{2}\mu^2 - 9\mu - \frac{35}{16} + \mu^4\right] R_+ = 0\end{aligned} \quad . \qquad (2)$$

An equivalent equation for the R_- component can be obtained from equation 2 by simply changing the sign of both μ and b_0 as well as replacing R_+ with R_-. This can be seen by inspection of system 1.

Equation 2 is a fourth order Hamburger equation (Ince, 1956) that can be solved explicitly using the Frobenius series technique as shown by Golding (2009, 2010). It has a regular singularity at the origin and an irregular singularity at ∞. The series approach is useful as an expansion around the regular singular point at the origin. However, the Frobenius technique cannot generally be used to find an expansion around the irregular singular point.

In equation 2, the equation for R_+ has been developed by eliminating R_- from the coupled equations in system 1. The behavior of the other spinor component is obtained from the following equation:

$$R_-(\rho) = \frac{1}{b_1\rho}\left\{\frac{d^2}{d\rho^2}R_+(\rho) + \frac{\frac{d}{d\rho}R_+(\rho)}{\rho} - \frac{\left(\mu+\frac{1}{2}\right)^2 R_+(\rho)}{\rho^2} + (\varepsilon+b_0)R_+(\rho)\right\} \tag{3}$$

that is easily obtained from the first equation in system 1.

In order to obtain useful information about the behavior of the solution as $\rho \to \infty$, an asymptotic expansion must be developed. This requires first the determination of the controlling factor and the leading behavior of the uncoupled fourth order equations.

4. Calculating the Controlling Factor and Leading Behavior

The first step in a solution of the asymptotic behavior of R_+ in equation 2 is to calculate the controlling factor of the expansion. This is done by assuming a trial solution of the form, $R_+ = \exp(S(\rho))$(Bender,1978). A differential equation for $S(\rho)$ is derived that must be approximately solved for large ρ. The full equation is

$$\begin{aligned}
&-\left(\frac{d}{d\rho}S(\rho)\right)^4 + \\
&\left(-6\frac{d^2}{d\rho^2}S(\rho) - 2\varepsilon + \frac{2\mu^2+5/2}{\rho^2}\right)\left(\frac{d}{d\rho}S(\rho)\right)^2 + \\
&\left(-4\frac{d^3}{d\rho^3}S(\rho) + 2\frac{b_0}{\rho} + \frac{-4\mu^2-6\mu-5}{\rho^3}\right)\frac{d}{d\rho}S(\rho) - \\
&3\left(\frac{d^2}{d\rho^2}S(\rho)\right)^2 + \left(-2\varepsilon + \frac{2\mu^2+5/2}{\rho^2}\right)\frac{d^2}{d\rho^2}S(\rho) - \\
&\frac{d^4}{d\rho^4}S(\rho) + b_1^2\rho^2 + b_0^2 - \varepsilon^2 + \\
&\frac{2\varepsilon\mu^2 - 2b_0\mu - 1/2\varepsilon - b_0}{\rho^2} + \left(9\mu - \mu^4 + \frac{35}{16} + 19/2\mu^2\right)\rho^{-4} = 0
\end{aligned} \tag{4}$$

By using the several approximations that $\frac{d^n}{d\rho^n}S << \left(\frac{d}{d\rho}S\right)^n$ as ρ gets large, the following simplified equation is obtained for $S(\rho)$,

$$\left(\frac{d}{d\rho}S(\rho)\right)^4 - 2\varepsilon\left(\frac{d}{d\rho}S(\rho)\right)^2 + b_1^2\rho^2 - \varepsilon^2 = 0 \tag{5}$$

.

By treating equation 5 as a quadratic equation in $\frac{d}{d\rho}S(\rho)$, the following four differential equations are derived:

$$\begin{aligned} \frac{dS}{d\rho} &= \pm i\sqrt{b_1\rho+\varepsilon}, \\ \frac{dS}{d\rho} &= \pm\sqrt{b_1\rho-\epsilon} \end{aligned} . \tag{6}$$

The solutions are

$$\begin{aligned} S(\rho) &= \pm\frac{2}{3b_1}\left(b_1\rho+\varepsilon\right)^{3/2} + C(\rho) \\ S(\rho) &= \pm i\frac{2}{3b_1}\left(b_1\rho-\varepsilon\right)^{3/2} + C(\rho) \end{aligned} \tag{7}$$

where $C(\rho)$ is an integration "constant" to be determined. The idea in the asymptotic analysis is that $C(\rho)$ should be much smaller at infinity than the first term in $S(\rho)$. Using the techniques described by Bender (1978), $C(\rho)$ is determined by substituting the solutions in equation 7 back into equation 4 and using the approximations that $\frac{d^n}{d\rho^n}C << \left(\frac{d}{d\rho}C\right)^n$ to obtain the leading behavior. By this technique, the factor $C(\rho)$ is found to be $-\frac{3}{4}\ln b_1\rho$ and the leading behavior is determined by the four functions

$$\frac{\exp\left(\frac{2\omega}{3b_1}\left(b_1\rho+\varepsilon\right)^{3/2}\right)}{\left(b_1\rho\right)^{3/4}} \tag{8}$$

in which the factor ω represent the four roots of unity, $\pm i, \pm 1$. To be consistent with the asymptotic nature of this calculation, the exponent is expanded and the terms that become small at large ρ are neglected. The factor $S(\rho)$ is then given by

$$S(\rho) \sim \frac{2\omega}{3b_1}\left(b_1\rho+\varepsilon\right)^{3/2} \sim 2\omega/3\sqrt{b_1}\left(\rho\right)^{3/2} + \omega\frac{\varepsilon\sqrt{\rho}}{\sqrt{b1}} . \tag{9}$$

This expansion of the exponent is consistent with the normal solutions at irregular singularities discussed by Ince (1956). However, this choice is not unique and other possible choices may or may not result in a consistent asymptotic series.

Using equation 9, the leading behavior of the radial wave function is given by the four functions that we refer to as the asymptotic basis functions

$$\frac{\exp\left(\omega\frac{2\sqrt{b_1}}{3}(\rho)^{3/2}+\omega\varepsilon\sqrt{\frac{\rho}{b_1}}\right)}{(b_1\rho)^{3/4}}. \tag{10}$$

The behavior of either spinor component, R_+ or R_- at large ρ must be asymptotic to some superposition of these four asymptotic basis functions. This is true even though the functions in equation 10 were derived from the equation for R_+, equation 2. The reason for this is that the equivalent fourth order equation for R_- only differs in the signs of μ and b_0, neither of which appear in equation 10. The leading factors for the two components are therefore identical. The actual dependence on μ and b_0 will reappear as more terms in the asymptotic expansion are included.

5. Stokes Phenomenon and the Asymptotic Basis Functions

In the global basis, all the physically allowed solutions found using the Frobenius technique in this problem are of the form (Golding, 2010)

$$\rho^{\sigma}\sum_{n=0}^{\infty}a_{2n}\rho^{2n}\ , \tag{11}$$

where σ is either an even or odd integer that depends only on the mode and component of interest. In the local basis, the components are superpositions of similar series of different indicial exponents σ and the analytic properties of the combined series are not as simple. For this reason, the global basis is used and the series form in equation 11 is taken as the general form for the asymptotic analysis below.

Once this series is extended to the complex plane by letting $\rho \to \rho e^{i\theta}$, the coefficients needed to combine the asymptotic basis functions of equation 10 into a proper approximation of the power series in equation 11 can be determined. This is accomplished by forcing both representations to have the same analytic properties for large ρ. The extension of the asymptotic basis functions to the complex plane are also obtained by the substitution $\rho \to \rho e^{i\theta}$ and are given by

$$\xi_{\omega}(\rho,\theta)=\frac{\exp\left(\frac{2\omega}{3b_1}(b_1\rho)^{3/2}\left(\cos\left(\frac{3\theta}{2}\right)+i\sin\left(\frac{3\theta}{2}\right)\right)\right)}{(b_1\rho)^{3/4}\,e^{i\frac{3\theta}{4}}},\ \text{where } \omega=\pm i,\ \pm 1. \tag{12}$$

The expression in equation 11 represents a single-valued function of θ in the complex plane. A reasonable approximation to this complex function at large values of ρ can be formed by using various linear combinations of the four asymptotic basis functions in equation 12 to create a single-valued function. However, the behavior of the individual basis functions in equation 12 is dramatically different in different sectors of the complex plane. Different linear combinations of the basis functions are required in each sector to approximate the series solutions. The different representations in each sector must in the end be matched to the adjoining sectors so that an effectively continuous function is formed. This matching process is handled using the phase integral techniques designed to deal with Stokes Phenomenon (Bender, 1978; Heading, 1962; White, 2005). The phase integral calculation takes place on the complex z-plane shown in figure 1. The basic technique is described in Heading (1962) and White (2005) for second order differential equations. In figure 1 the lines described as anti-Stokes lines radiate outwards along the lines $\theta = 0, \pm\frac{2\pi}{3}$. These lines cut the plane up into three sectors where different forms of the solution are used.

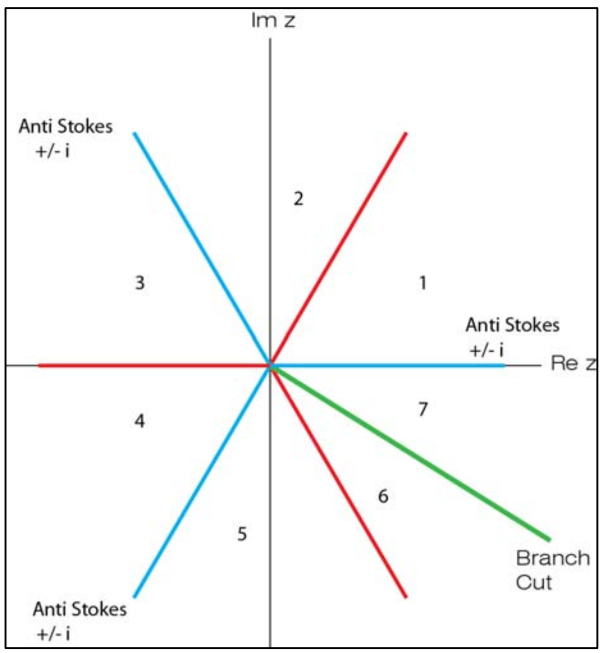

Figure 1. Complex plane showing the positions of the anti-Stokes lines needed to perform the phase integral calculation that properly combines the asymptotic basis functions.

The anti-Stokes lines are defined so that the pair of exponential solutions with $\omega = \pm i$ in equation 12 have pure imaginary phase and therefore do not decay towards infinity. Along another set of lines called the Stokes lines (the red lines in figure 1) these same oscillatory solutions have purely real exponents and one solution decays towards infinity while the other grows exponentially. The real component of the phase changes sign on crossing an anti-Stokes line. Thus, an exponentially growing solution in one sector abruptly becomes an exponentially

decaying solution in the adjacent sector. Phase integral techniques are intended to smooth out this apparent discontinuity.

An important consideration in this problem is that there are four functions in equation 12 that must be considered. These functions form two pairs and the Stokes lines of one pair are the anti-Stokes lines of the other pair. For example, along the real axis where $\theta = 0$, the solutions with $\omega = \pm i$ have purely imaginary phase and thus do not decay towards infinity while the solutions with $\omega = \pm 1$ have purely real phase and break up into decaying and growing exponentials.

The calculation proceeds by starting in sector 7 of figure 1 with a superposition of the form $A\xi_{+i}^{d} + B\xi_{-i}^{s} + C\xi_{+1}^{d} + D\xi_{-1}^{s}$ ($A, B, C,$ and D are assumed to be complex constants). The superscripts s and d refer to the subdominant or dominant nature of the basis function in the sector. Subdominant components decay towards infinity and dominant components grow.

The first step is to determine a superposition in region 1 that is consistent with the assumed form in region 7. This is accomplished using arbitrary Stokes constants and by adjusting the dominancy of the solutions as described in both Heading (1962) and White (2005). Since the phase factor in the denominator of the basis functions is independent of ρ, it can be ignored except when crossing the branch cut. Once this process is complete the solution in region 2 is developed from that in region using the Stokes constant, T_1. This process proceeds around the complex plane until after dealing with the branch cut, region 7 is reached again. Referring to the diagram in figure 1 the detailed calculation goes as follows:

1. Starting in region 7 with the assumed form $A\xi_{+i}^{d} + B\xi_{-i}^{s} + C\xi_{+1}^{d} + D\xi_{-1}^{s}$
2. Cross into region 1 obtaining $A\xi_{+i}^{s} + B\xi_{-i}^{d} + C\xi_{+1}^{d} + \left(D + T_1 C\right)\xi_{-1}^{s}$
3. Cross into region 2 obtaining $\left(A + T_2 B\right)\xi_{+i}^{s} + B\xi_{-i}^{d} + C\xi_{+1}^{s} + \left(D + T_1 C\right)\xi_{-1}^{d}$
4. Cross into region 3 obtaining $\left(A + T_2 B\right)\xi_{+i}^{d} + B\xi_{-i}^{s} + \left(C + T_3\left(D + T_1 C\right)\right)\xi_{+1}^{s} + \left(D + T_1 C\right)\xi_{-1}^{d}$
5. Cross into region 4 obtaining
   $\left(A + T_2 B\right)\xi_{+i}^{d} + \left(B + T_4\left(A + T_2 B\right)\right)\xi_{-i}^{s} + \left(C + T_3\left(D + T_1 C\right)\right)\xi_{+1}^{d} + \left(D + T_1 C\right)\xi_{-1}^{s}$
6. Cross into region 5 obtaining
   $\left(A + T_2 B\right)\xi_{+i}^{s} + \left(B + T_4\left(A + T_2 B\right)\right)\xi_{-i}^{d} +$
   $\left(C + T_3\left(D + T_1 C\right)\right)\xi_{+1}^{d} + \left(\left(D + T_1 C\right) + T_5\left(C + T_3\left(D + T_1 C\right)\right)\right)\xi_{-1}^{s}$
7. Cross into region 6 obtaining
   $\left(\left(A + T_2 B\right) + T_6\left(B + T_4\left(A + T_2 B\right)\right)\right)\xi_{+i}^{s} + \left(B + T_4\left(A + T_2 B\right)\right)\xi_{-i}^{d} +$
   $\left(C + T_3\left(D + T_1 C\right)\right)\xi_{+1}^{s} + \left(\left(D + T_1 C\right) + T_5\left(C + T_3\left(D + T_1 C\right)\right)\right)\xi_{-1}^{d}$
8. Cross the branch cut to get back to region 7 obtaining
   $+i\left(\left(A + T_2 B\right) + T_6\left(B + T_4\left(A + T_2 B\right)\right)\right)\xi_{-i}^{s} + i\left(B + T_4\left(A + T_2 B\right)\right)\xi_{+i}^{d} +$
   $i\left(C + T_3\left(D + T_1 C\right)\right)\xi_{-1}^{s} + i\left(\left(D + T_1 C\right) + T_5\left(C + T_3\left(D + T_1 C\right)\right)\right)\xi_{+1}^{d}$

At this point there are two different descriptions of the function in region 7 that can be made equal by calculating consistent values of the Stokes constants. By this process there is essentially a different description of the desired function in each region of the plane and these functions must all be connected together so that the patched representation of the function in equation 11 is as continuous and singled valued as possible. By comparing the final expression obtained in region 7 with the expression that began the calculation in region 7, four equations are obtained that are sufficient to determine that all of the Stokes constants, T_i are equal to $-i$.

Once the Stokes constants are evaluated then the behavior of the total solution in the various regions can be used to completely calculate the required relations between the amplitudes, A, B, C, D, of the asymptotic basis functions needed to properly approximate the asymptotic behavior of the series solutions of equation 11.

As noted before, the series in equation 11 implies that the extended function along the negative real axis must be equal to $e^{i\sigma\pi}$ times the function along the positive real axis. Setting all of the Stokes constants equal to $-i$ and ignoring appropriate subdominant terms that decay exponentially along the real axis, the expression along the negative real axis in region 1 becomes $\left(A-iB\right)\xi_{+i}^{d}-iD\xi_{+1}^{s}+\left(D-iC\right)\xi_{-1}^{d}$ and the similar expression along the positive real axis is $A\xi_{+i}^{s}+B\xi_{-i}^{d}+C\xi_{+1}^{d}$. Taking all of this into account and including the phase shift, $e^{-i\frac{3\pi}{4}}$ common to all of the basis functions evaluated along the negative real axis, the following equation is obtained:

$$\begin{gathered}e^{i\sigma\pi}\left[A\exp\left(\frac{2i}{3b_1}\left(b_1\rho\right)^{3/2}\right)+B\exp\left(-\frac{2i}{3b_1}\left(b_1\rho\right)^{3/2}\right)+C\exp\left(\frac{2}{3b_1}\left(b_1\rho\right)^{3/2}\right)\right]=\\ e^{-i\frac{3\pi}{4}}\left[\left(A-iB\right)\exp\left(\frac{2}{3b_1}\left(b_1\rho\right)^{3/2}\right)-iD\exp\left(-\frac{2i}{3b_1}\left(b_1\rho\right)^{3/2}\right)+\left(D-iC\right)\exp\left(\frac{2i}{3b_1}\left(b_1\rho\right)^{3/2}\right)\right]\end{gathered}. \quad (13)$$

Equating the coefficients of common basis functions in this expression the relations

$$\begin{gathered}\left(A-iB\right)e^{-i\frac{3\pi}{4}}=e^{i\sigma\pi}C\\ -iDe^{-i\frac{3\pi}{4}}=e^{i\sigma\pi}B \qquad ,\\ \left(D-iC\right)e^{-i\frac{3\pi}{4}}=e^{i\sigma\pi}A\end{gathered} \quad (14)$$

are found. The eigenfunctions described by the series in equation 11 must be finite and real valued along the positive real axis. This is enough information to determine that the coefficients are given by

$$
\begin{aligned}
&A = \pm |A| e^{i\frac{\pi}{4}} \\
&B = \pm |A| e^{-i\frac{\pi}{4}} \\
&C = 0 \\
&D = \mp |A| e^{i\sigma\pi}
\end{aligned} \qquad (15)
$$

The two possible sets of solutions are necessary to account for the sign of the exponentially decaying components of the radial eigenfunctions as the radial mode number is increased. That is, if the lowest energy eigenfunction of a particular mode has no zero crossings then D is taken to be positive allowing the bound component of the wavefunction to decay from positive values towards zero. If σ is odd the upper sign is taken and if σ is even the lower sign must be taken. The next higher radial mode would require D to be negative.

6. Results of Phase Integral Calculations

Using the constants determined by the phase integral technique the functional forms of the leading behavior for each component and each mode are displayed here:

$$
\begin{aligned}
R_{p1} &= 2\frac{\cos\left(\frac{2}{3}\sqrt{b_1}\rho^{3/2} + \varepsilon\sqrt{\rho / b_1} + \frac{\pi}{4}\right)}{\left(b_1\rho\right)^{3/4}} - \left(-1\right)^{\mu+5/2} \frac{\mathrm{e}^{-\frac{2}{3}\sqrt{b_1}\rho^{3/2} + \varepsilon\sqrt{\rho/b_1}}}{\left(b_1\rho\right)^{3/4}} \\
R_{m1} &= -2\frac{\cos\left(\frac{2}{3}\sqrt{b_1}\rho^{3/2} + \varepsilon\sqrt{\rho / b_1} + \frac{\pi}{4}\right)}{\left(b_1\rho\right)^{3/4}} - \left(-1\right)^{\mu+5/2} \frac{\mathrm{e}^{-\frac{2}{3}\sqrt{b_1}\rho^{3/2} + \varepsilon\sqrt{\rho/b_1}}}{\left(b_1\rho\right)^{3/4}} \\
R_{m2} &= -2\frac{\cos\left(\frac{2}{3}\sqrt{b_1}\rho^{3/2} + \varepsilon\sqrt{\rho / b_1} + \frac{\pi}{4}\right)}{\left(b_1\rho\right)^{3/4}} + \left(-1\right)^{\mu+7/2} \frac{\mathrm{e}^{-\frac{2}{3}\sqrt{b_1}\rho^{3/2} + \varepsilon\sqrt{\rho/b_1}}}{\left(b_1\rho\right)^{3/4}} \\
R_{p2} &= 2\frac{\cos\left(\frac{2}{3}\sqrt{b_1}\rho^{3/2} + \varepsilon\sqrt{\rho / b_1} + \frac{\pi}{4}\right)}{\left(b_1\rho\right)^{3/4}} + \left(-1\right)^{\mu+7/2} \frac{\mathrm{e}^{-\frac{2}{3}\sqrt{b_1}\rho^{3/2} + \varepsilon\sqrt{\rho/b_1}}}{\left(b_1\rho\right)^{3/4}}
\end{aligned} . \qquad (16)
$$

These four functions represent the leading behavior of the spinor components and are valid along the positive real axis as $\rho \to \infty$. The proportionality factor $|A|$ has been set equal to one as these solutions need to be matched to series solutions describing the behavior in the area of the origin.

The functions, R_{p1} and R_{p2}, refer to the spin-up components of type 1 modes and type 2 modes (Golding, 2009) and R_{m1} and R_{m2} similarly refer to the associated spin-down components. The phase choice in these expressions produces a positive decaying exponential for the tail of the bound component of the ground state for $\mu = 1/2$. The overall phase is unimportant but the relative phase between the cosine and exponential terms in each function is the mathematical cause of the exponential decay normally seen in the bound state components, $R_p + R_m$. A quick check shows that the sinusoidal terms cancel out in the bound components and the exponentials cancel out when the difference components, $R_p - R_m$ are calculated. Thus each of the global spinor components, R_p, R_m shown in equation 12 contains a mixture of an unbound and a bound component.

Within a given series of radial eigenfunctions the boundary conditions are identical for each mode at the center of the guide. As the eigenenergies increase from one radial mode to the next, the sign of the exponential factor must change to account for the increasing number of zero crossing at higher energies. This can be handled by multiplying each of the functions in equation 12 by a factor, -1^{n_1} or -1^{n_2}, the new parameters, n_1 and n_2, are then the radial mode indices for the radial wavefunctions. These factors are not included above but can be easily included when working with a full set of modes.

7. Asymptotic Expansion of the Mode Functions

In order to obtain a more accurate form of the mode functions than just the leading behavior shown in equation 16, a full asymptotic expansion must be calculated. This is accomplished by solving equation 2 using an assumed form that is made up of the product of the leading behavior of the mode times a series consisting of inverse powers of ρ. The coefficients of the series expansion are then determined recursively by equating the factors multiplying each power of ρ in the resulting series zero.

Substituting the following expansion in equation 2,

$$R_{+}(\rho) = w_1(\rho)\frac{\cos\left(\frac{2}{3}\sqrt{b_1}\rho^{3/2} + \varepsilon\sqrt{\rho/b_1}\right)}{(b_1\rho)^{3/4}} + w_2(\rho)\frac{\sin\left(\frac{2}{3}\sqrt{b_1}\rho^{3/2} + \varepsilon\sqrt{\rho/b_1}\right)}{(b_1\rho)^{3/4}} \qquad (17)$$

results in a set of coupled differential equations for w_1 and w_2 that can be solved by assuming that these functions have the following asymptotic expansions:

$$w_1 = \sum_{n=0}^{\infty} a_i \rho^{-n/2} \text{ and } w_2 = \sum_{n=0}^{\infty} c_i \rho^{-n/2} . \qquad (18)$$

Solving the resulting coupled series expansions for the first few coefficients results in the following approximate form for w_1 when $b_0 = 0$:

$$
\begin{aligned}
w_1 \sim\ & a_0 + \left(1/4\frac{\varepsilon^2}{b_1^{3/2}} - 1/2\frac{b_0^{\ 2}}{b_1^{3/2}}\right)\frac{c_0}{\sqrt{\rho}} + \\
& \left(-1/4\frac{\varepsilon}{b_1} + 1/2\frac{b_0}{b_1} - 1/32\frac{\varepsilon^4}{b_1^{\ 3}} + 1/8\frac{\varepsilon^2 b_0^{\ 2}}{b_1^{\ 3}} - 1/8\frac{b_0^{\ 4}}{b_1^{\ 3}}\right)\frac{a_0}{\rho} + \\
& \left(\begin{array}{l} -\frac{1}{384}\frac{\varepsilon^6}{b_1^{9/2}} + \frac{1}{64}\frac{\varepsilon^4 b_0^{\ 2}}{b_1^{9/2}} - \frac{5}{48}\frac{\varepsilon^3}{b_1^{5/2}} + \left(1/8\frac{b_0}{b_1^{5/2}} - 1/32\frac{b_0^{\ 4}}{b_1^{9/2}}\right)\varepsilon^2 + \\ \frac{5}{24}\frac{\varepsilon b_0^{\ 2}}{b_1^{5/2}} + \left(-\frac{5}{48} + 1/3\mu^2\right)\left(\sqrt{b_1}\right)^{-1} - 1/4\frac{b_0^{\ 3}}{b_1^{5/2}} + 1/48\frac{b_0^{\ 6}}{b_1^{9/2}} \end{array}\right)\frac{c_0}{\rho^{3/2}} + \\
& \left(\begin{array}{l} \frac{1}{6144}\frac{\varepsilon^8}{b_1^{\ 6}} - \frac{1}{768}\frac{\varepsilon^6 b_0^{\ 2}}{b_1^{\ 6}} + \frac{7}{384}\frac{\varepsilon^5}{b_1^{\ 4}} + \left(-\frac{1}{64}\frac{b_0}{b_1^{\ 4}} + \frac{1}{256}\frac{b_0^{\ 4}}{b_1^{\ 6}}\right)\varepsilon^4 - \\ \frac{7}{96}\frac{\varepsilon^3 b_0^{\ 2}}{b_1^{\ 4}} + \left(\left(\frac{35}{192} - 1/12\mu^2\right)b_1^{-2} + 1/16\frac{b_0^{\ 3}}{b_1^{\ 4}} - \frac{1}{192}\frac{b_0^{\ 6}}{b_1^{\ 6}}\right)\varepsilon^2 + \\ \left(-1/8\frac{b_0}{b_1^{\ 2}} + \frac{7}{96}\frac{b_0^{\ 4}}{b_1^{\ 4}}\right)\varepsilon + \left(1/6\mu^2 - \frac{29}{96}\right)b_0^{\ 2}b_1^{-2} - 1/16\frac{b_0^{\ 5}}{b_1^{\ 4}} + \frac{1}{384}\frac{b_0^{\ 8}}{b_1^{\ 6}} \end{array}\right)\frac{a_0}{\rho^2} + \cdots
\end{aligned}
\tag{19}
$$

and the corresponding form for w_2

$$w_2 \sim c_0 - \left(1/4\frac{\varepsilon^2}{b_1^{3/2}} - 1/2\frac{b_0^{\ 2}}{b_1^{3/2}}\right)\frac{a_0}{\sqrt{\rho}} +$$
$$\left(-1/4\frac{\varepsilon}{b_1} + 1/2\frac{b_0}{b_1} - 1/32\frac{\varepsilon^4}{b_1^{\ 3}} + 1/8\frac{\varepsilon^2 b_0^{\ 2}}{b_1^{\ 3}} - 1/8\frac{b_0^{\ 4}}{b_1^{\ 3}}\right)\frac{c_0}{\rho} -$$
$$\left(\begin{array}{l} -\frac{1}{384}\frac{\varepsilon^6}{b_1^{9/2}} + \frac{1}{64}\frac{\varepsilon^4 b_0^{\ 2}}{b_1^{9/2}} - \frac{5}{48}\frac{\varepsilon^3}{b_1^{5/2}} + \left(1/8\frac{b_0}{b_1^{5/2}} - 1/32\frac{b_0^{\ 4}}{b_1^{9/2}}\right)\varepsilon^2 + \\ \frac{5}{24}\frac{\varepsilon b_0^{\ 2}}{b_1^{5/2}} + \left(-\frac{5}{48} + 1/3\mu^2\right)\left(\sqrt{b_1}\right)^{-1} - 1/4\frac{b_0^{\ 3}}{b_1^{5/2}} + 1/48\frac{b_0^{\ 6}}{b_1^{9/2}} \end{array}\right)\frac{a_0}{\rho^{3/2}} +$$
$$\left(\begin{array}{l} \frac{1}{6144}\frac{\varepsilon^8}{b_1^{\ 6}} - \frac{1}{768}\frac{\varepsilon^6 b_0^{\ 2}}{b_1^{\ 6}} + \frac{7}{384}\frac{\varepsilon^5}{b_1^{\ 4}} + \left(-\frac{1}{64}\frac{b_0}{b_1^{\ 4}} + \frac{1}{256}\frac{b_0^{\ 4}}{b_1^{\ 6}}\right)\varepsilon^4 - \\ \frac{7}{96}\frac{\varepsilon^3 b_0^{\ 2}}{b_1^{\ 4}} + \left(\left(\frac{35}{192} - 1/12\mu^2\right)b_1^{-2} + 1/16\frac{b_0^{\ 3}}{b_1^{\ 4}} - \frac{1}{192}\frac{b_0^{\ 6}}{b_1^{\ 6}}\right)\varepsilon^2 + \\ \left(-1/8\frac{b_0}{b_1^{\ 2}} + \frac{7}{96}\frac{b_0^{\ 4}}{b_1^{\ 4}}\right)\varepsilon + \left(1/6\mu^2 - \frac{29}{96}\right)b_0^{\ 2}b_1^{-2} - 1/16\frac{b_0^{\ 5}}{b_1^{\ 4}} + \frac{1}{384}\frac{b_0^{\ 8}}{b_1^{\ 6}} \end{array}\right)\frac{c_0}{\rho^2} + \cdots \tag{20}$$

In this section, some of longer expressions are written in stacked forms within parentheses to try and clarify the expressions. Do not confuse these expressions with matrices as they are to be read as a single series of terms. In order to maintain the leading behavior form found by the phase integral technique in equation 16, the coefficients, a_0 and c_0, must be chosen to produce the $\frac{\pi}{4}$ phase shift in the cosine terms shown in equation 16. This is easily accomplished by setting the first coefficient, $a_0 = \frac{1}{\sqrt{2}}$, and the second coefficient, $c_0 = -\frac{1}{\sqrt{2}}$.

The first few terms of the asymptotic expansion of R_+ are then

$$\begin{array}{l} R_+ \sim \frac{\cos\left(\frac{2}{3}\sqrt{b_1}\rho^{3/2} + \varepsilon\sqrt{\rho/b_1}\right)}{\left(b_1\rho\right)^{3/4}}\left(\frac{1}{\sqrt{2}} - \left(1/4\frac{\varepsilon^2}{b_1^{3/2}} - 1/2\frac{b_0^{\ 2}}{b_1^{3/2}}\right)\frac{1}{\sqrt{2\rho}}\right) + \\ \frac{\sin\left(\frac{2}{3}\sqrt{b_1}\rho^{3/2} + \varepsilon\sqrt{\rho/b_1}\right)}{\left(b_1\rho\right)^{3/4}}\left(-\frac{1}{\sqrt{2}} - \left(1/4\frac{\varepsilon^2}{b_1^{3/2}} - 1/2\frac{b_0^{\ 2}}{b_1^{3/2}}\right)\frac{1}{\sqrt{2\rho}}\right) \end{array}. \tag{21}$$

Ignoring the second term in each bracket as $\rho \to \infty$, the expression reduces to the form found in equation 16 along with the $\frac{\pi}{4}$ phase factor that comes from combining the $\sin$ and the $\cos$ terms. Similar expansions are found for the other components and the other modes of the guide.

An expansion for the purely exponential term shown in equation 16 can also be included by straightforward extension of the trial function shown in equation 17 to include an exponential times another asymptotic series, $w_3(\rho)$. Since the exponential dies off so quickly this is only important for an asymptotic representation of the atomic wavefunction relatively near to the center of the guide yet outside the classical turning point of the mode of interest.

To attain good accuracy, a significant number of terms are needed in the asymptotic expansions. However, the expressions are long and difficult to display so only a few terms are shown here. The unbound component is the component that is pointed in the direction of the local magnetic field. This component sees the magnetic potential energy decreasing towards infinity and is repelled from the center of the guide. The unbound component is given by $R_+(\rho)-R_-(\rho)$. It decays fairly slowly, is not extremely sensitive to the bias field, b_0 and the first few terms of its expansion are displayed in equation 22,

$$\begin{aligned}
&R_+ - R_- \sim \\
&\cos\left(\frac{2}{3}\sqrt{b_1}\rho^{3/2}+\varepsilon\sqrt{\rho/b_1}\right)\left[\begin{array}{l}\dfrac{\sqrt{2}}{b_1^{3/4}\rho^{3/4}}+\dfrac{1/2\sqrt{2}b_0^{\,2}-1/4\sqrt{2}\varepsilon^2}{b_1^{9/4}\rho^{5/4}}+\\ \left(-1/4\dfrac{\sqrt{2}\epsilon}{b_1^{7/4}}+\left(-1/8\sqrt{2}b_0^{\,4}+1/8\sqrt{2}\varepsilon^2 b_0^{\,2}-1/32\sqrt{2}\varepsilon^4\right)b_1^{-\frac{15}{4}}\right)\rho^{-7/4}\end{array}\right]+ \qquad (22)\\
&\sin\left(\frac{2}{3}\sqrt{b_1}\rho^{3/2}+\varepsilon\sqrt{\rho/b_1}\right)\left[\begin{array}{l}-\dfrac{\sqrt{2}}{b_1^{3/4}\rho^{3/4}}+\dfrac{1/2\sqrt{2}b_0^{\,2}-1/4\sqrt{2}\varepsilon^2}{b_1^{9/4}\rho^{5/4}}+\\ \left(1/4\dfrac{\sqrt{2}\varepsilon}{b_1^{7/4}}+\left(1/8\sqrt{2}b_0^{\,4}-1/8\sqrt{2}\varepsilon^2 b_0^{\,2}+1/32\sqrt{2}\varepsilon^4\right)b_1^{-\frac{15}{4}}\right)\rho^{-7/4}\end{array}\right]
\end{aligned}$$

The other interesting component for any mode is the bound component. This is given by $R_+(\rho)+R_-(\rho)$, which decays exponentially except for a small oscillatory component in the tail given by equation 23 when the bias field, b_0 is zero,

$$\begin{aligned}
&R_+ + R_- \sim \\
&\cos\left(\frac{2}{3}\sqrt{b_1}\rho^{3/2}+\varepsilon\sqrt{\rho/b_1}\right)\left[-1/2\sqrt{2}\mu b_1^{-7/4}\rho^{-\frac{15}{4}}+1/8\sqrt{2}\varepsilon^2\mu b_1^{-\frac{13}{4}}\rho^{-\frac{17}{4}}\right]+ \qquad (23)\\
&\sin\left(\frac{2}{3}\sqrt{b_1}\rho^{3/2}+\varepsilon\sqrt{\rho/b_1}\right)\left[1/2\sqrt{2}\mu b_1^{-7/4}\rho^{-\frac{15}{4}}+1/8\sqrt{2}\varepsilon^2\mu b_1^{-\frac{13}{4}}\rho^{-\frac{17}{4}}\right]
\end{aligned}$$

Notice that this oscillating term drops off like $\dfrac{1}{\rho^{15/4}}$ and is proportional to the alignment.

However, when the bias field is increased there is a pronounced effect on the behavior of the oscillatory terms that make up the bound component as can be seen in equation 24,

$$
\begin{aligned}
R_{+} + R_{-} \sim\ & \cos\left(\frac{2}{3}\sqrt{b_1}\rho^{3/2} + \varepsilon\sqrt{\rho / b_1}\right)\left[\begin{array}{l}
1/2\dfrac{\sqrt{2}b_0}{b_1^{7/4}\rho^{7/4}} + \dfrac{1}{196608}\sqrt{2}\left(49152 b_1^{6} b_0^{3} - 24576 b_1^{6} b_0 \varepsilon^{2}\right) b_1^{-\frac{37}{4}}\rho^{-9/4} + \\
\dfrac{1}{196608}\sqrt{2}\begin{pmatrix} -24576 b_1^{13/2}\varepsilon b_0 - 12288 b_1^{9/2} b_0^{5} + \\ 12288 b_1^{9/2}\varepsilon^{2} b_0^{3} - 3072 b_1^{9/2} b_0 \epsilon^{4} \end{pmatrix} b_1^{-\frac{37}{4}}\rho^{-11/4} + \\
\dfrac{1}{196608}\sqrt{2}\begin{pmatrix} -20480 b_1^{5}\varepsilon b_0^{3} + 256 b_1^{3}\epsilon^{6} b_0 + 108544 b_1^{7} b_0 - \\ 32768 b_1^{7}\mu^{2} b_0 + 3072 b_1^{3}\varepsilon^{2} b_0^{5} - 2048 b_1^{3} b_0^{7} + \\ 10240 b_1^{5}\varepsilon^{3} b_0 - 1536 b_1^{3}\varepsilon^{4} b_0^{3} \end{pmatrix} b_1^{-\frac{37}{4}}\rho^{-\frac{13}{4}}
\end{array}\right] + \\
& \sin\left(\frac{2}{3}\sqrt{b_1}\rho^{3/2} + \varepsilon\sqrt{\rho / b_1}\right)\left[\begin{array}{l}
-1/2\dfrac{\sqrt{2}b_0}{b_1^{7/4}\rho^{7/4}} + \dfrac{1}{196608}\sqrt{2}\left(49152 b_1^{6} b_0^{3} - 24576 b_1^{6} b_0 \varepsilon^{2}\right) b_1^{-\frac{37}{4}}\rho^{-9/4} + \\
\dfrac{1}{196608}\sqrt{2}\begin{pmatrix} -12288 b_1^{9/2}\varepsilon^{2} b_0^{3} + 3072 b_1^{9/2} b_0 \varepsilon^{4} + \\ 24576 b_1^{13/2}\varepsilon b_0 + 12288 b_1^{9/2} b_0^{5} \end{pmatrix} b_1^{-\frac{37}{4}}\rho^{-11/4} + \\
\dfrac{1}{196608}\sqrt{2}\begin{pmatrix} -20480 b_1^{5}\varepsilon b_0^{3} + 256 b_1^{3}\varepsilon^{6} b_0 + 108544 b_1^{7} b_0 - \\ 32768 b_1^{7}\mu^{2} b_0 + 3072 b_1^{3}\varepsilon^{2} b_0^{5} - 2048 b_1^{3} b_0^{7} + \\ 10240 b_1^{5}\varepsilon^{3} b_0 - 1536 b_1^{3}\varepsilon^{4} b_0^{3} \end{pmatrix} b_1^{-\frac{37}{4}}\rho^{-\frac{13}{4}}
\end{array}\right].
\end{aligned}
\tag{24}
$$

All of the terms displayed in equation 24 are proportional to the bias field, b_0 and vanish at zero bias. Note also that the radial dependence is much stronger in these bias dependent components. These effects are small at low bias fields but are expected to become important when studying the adiabatic problem when it is normal to include large bias fields to eliminate the possibility of some types of spin flips.

---

8. Conclusions

A method for calculating complete asymptotic expansions for the modes of atomic waveguides has been demonstrated. The technique can be extended to high orders using computer algebra techniques. This method complements the series solution technique presented in Golding (2010) and produces an accurate representation of the waveguide solutions far away from the guide center.

In this system, some components of the spinor wavefunctions do not die off exponentially and are therefore significant at large distances. This is related to the quasibound nature of the system.

A good representation of the nondecaying components of the eigenstates at large distances from the guide center is required so that the calculated eigenstates can be used reliably in further numerical calculations. The asymptotic expansions presented here provide this representation and are readily related to the power series solutions developed in Golding (2010). By connecting those power series solutions to the asymptotic expansions developed here an efficient representation of the exact radial wavefunctions can be obtained. These wavefunctions are needed for detailed studies of important properties of magnetic guides such as sensitivity to noise driven spin flips, importance of quantum Majorana transitions, energy level dependence on magnetic field, and the effects of guiding field imperfections as well as the onset and departure of adiabatic behavior.

9. References

Bender, C. M.; Orszag, S. A. *Advanced Mathematical Methods for Scientists and Engineers*; McGraw-Hill: New York, NY, 1978.

Brink, D. M.; Sukumar, C. V. *Phys. Rev. A 75* **2006**, 035401.

Golding, W. M. *Atomic Waveguides for Atom Chips*; ARL-TR-5014; U.S. Army Research Laboratory: Adelphi, MD, Oct. 2009.

Golding, W. M. *Series Solutions for Atom Guides*; ARL-TR-5335; U.S. Army Research Laboratory: Adelphi, MD, Sept. 2010.

Heading, J. *An Introduction to Phase-Integral Methods*; Metheun: New York, NY, 1962.

Hinds, E. A.; Eberlein, C. *Phys. Rev. A 61* **2000**, 033614.Ince, E. L. *Ordinary Differential Equations;* Dover: New York, NY, 1956, p. 396.

Lesanovsky, I.; Schmelcher, P. *Phys. Rev. A 70* **2004**, 063604.

Potvliege, R.M. and Zehnlé, V. *Phys. Rev. A 63*, **2001**, 025601.

Sukumar, C. V.; Brink, D. M. *Phys. Rev. A 56* **1997**, 2451.

White, Roscoe B., *Asymptotic Analysis of Differential Equations*; Imperial College Press: London, 2005, p. 67.

NO. OF COPIES	ORGANIZATION
1 PDF	DEFENSE TECH INFO CTR ATTN DTIC OCA 8725 JOHN J KINGMAN RD STE 0944 FT BELVOIR VA 22060-6218
1 CD	OFC OF THE SECY OF DEFNS ATTN ODDRE (R&AT) THE PENTAGON WASHINGTON DC 20301-3080
1	US ARMY RSRCH DEV AND ENGRG CMND ARMAMENT RSRCH DEV & ENGRG CTR ARMAMENT ENGRG & TECHNLGY CTR ATTN AMSRD AAR AEF T J MATTS BLDG 305 ABERDEEN PROVING GROUND MD 21005-5001
1	PM TIMS, PROFILER (MMS-P) AN/TMQ-52 ATTN B GRIFFIES BUILDING 563 FT MONMOUTH NJ 07703
1	US ARMY INFO SYS ENGRG CMND ATTN AMSEL IE TD A RIVERA FT HUACHUCA AZ 85613-5300
1	COMMANDER US ARMY RDECOM ATTN AMSRD AMR W C MCCORKLE 5400 FOWLER RD REDSTONE ARSENAL AL 35898-5000
3	DEPT OF THE ARMY WEAPONS SCIENCES DIRECTORATE ATTN AMSRD AMS WS H EVERITT ATTN AMSRD AMS WS K MYNENI ATTN AMSRD AMS WS T BAHDER REDSTONE ARSENAL AL 35898-5000
1	US GOVERNMENT PRINT OFF DEPOSITORY RECEIVING SECTION ATTN MAIL STOP IDAD J TATE 732 NORTH CAPITOL ST NW WASHINGTON DC 20402

NO. OF COPIES	ORGANIZATION
1	US ARMY RSRCH LAB ATTN RDRL CIM G T LANDFRIED BLDG 4600 ABERDEEN PROVING GROUND MD 21005-5066
1 HC 1 CD	US ARMY RSRCH OFC ATTN P REYNOLDS PO BOX 12211 RESEARCH TRIANGLE PARK NC 27709-2211
29	US ARMY RSRCH LAB ATTN IMNE ALC HRR MAIL & RECORDS MGMT ATTN RDRL CIM L TECHL LIB ATTN RDRL CIM P TECHL PUB ATTN RDRL SEE O N FELL ATTN RDRL SEE O P LEE ATTN RDRL SEE O P PELLEGRINO ATTN RDRL SEE O W M GOLDING (20 COPIES) ATTN RDRL SER E F CROWNE ATTN RDRL SES E H BRANDT ATTN RDRL SES P A EDELSTEIN ADELPHI MD 20783-1197
TOTAL:	42 (39 HCS, 2 CDS, 1 PDF)